Bulk Plasma Impurity Behaviour with the new JET Configuration

R Barnsley[1], H Chen[2], I H Coffey[4], D Cushing, R Giannella, L Lauro-Taroni, K D Lawson[3], P McGinnity[4], N J Peacock[3], M Singleton[5], M von Hellermann

JET Joint Undertaking, OX14 3EA.
1 Leicester University, LE1 7RH, 2 Southwestern Institute of Physics, Chengdu, China.
3 AEA Culham Laboratory, OX14 3DB, 4 Queens University, Belfast, BT7 1NN.
5 Cork University, Republic of Ireland.

Introduction

Bulk plasma impurities were monitored by VUV, XUV and soft x-ray spectroscopy, with an emphasis on obtaining quantitative data. Absolutely-calibrated line intensities have been modelled, with the aim of deriving impurity concentrations by passive spectroscopy. Impurity radiated power components, derived by fitting line intensities to the total radiated power, have been used to monitor impurities both during discharges and over long sequences of discharges.

Experimental

From the beginning of operations in 1994, impurities were monitored by a broad-band soft x-ray spectrometer /1/. This was a valuable complement to the VUV/XUV grating instruments, and has the advantages for quantitative measurements that it can be absolutely calibrated, and can measure the continuum. It uses a combination of crystals and synthetic multilayers to cover almost completely the spectrum between 0.3nm and 10nm, and monitors the main impurities under all discharge conditions, including D-T discharges /2/. The sensitivity function is synthesised from the instrument sensitivity equation by a computer code. This contains details of the instrument geometry, mass absorption coefficients for the window materials and detector gas mixture, and measured or theorectical diffractor data as available. The essential characterisation of Bragg diffractors is being continued /3/, particularly for synthetic multilayers, and to assess radiation damage.

Simulation of calibrated line intensities

The determination of impurity concentrations from central-chord passive spectroscopy is a severe problem, particularly for the light impurities that usually dominate the fuel dilution in devices with low-Z limiters. Some progress has been made here by modelling soft x-ray line intensities with the SANCO impurity transport code. Using data from divertor gas-puffing experiments, transport parameters were derived by modelling the impurity profiles measured by CXRS.

Either neon or nitrogen were puffed into ELMy H-modes with typically 10MW of neutral-beam heating. The light impurity abundance profiles measured by CXRS were hollow, with the peak at about r/a=0.75, and were modelled with profiles of the transport coefficients D and V shown in figure 1. These transport profiles are characterised in the centre by low diffusion and a small outward convection, and near the edge by moderate diffusion and strong inward convection. The Neon X Lyβ measurement and simulation shown in figure 2, are independent of each other in that the simulation is based solely on CXRS measurements, while the measurement is the absolutely calibrated soft x-ray line intensity. The peak CXRS Neon concentration was about 0.4% of n_e at r/a=0.75, the Ne-

Lyβ measurement being about 40% lower than the simulation. Using similar data from a nitrogen puff, the simulation predicted a peak nitrogen concentration of 10% of n_e at r/a=0.4: approximately twice the CXRS value at the same radius. Given the cumulative uncertainties inherent in this comparison, estimated to total at least a factor two, the present level of agreement is considered to be good, with the possibility of extending passive measurements to other impurities, and to non-beam-heated discharges.

Impurity behaviour

The technique of deriving impurity radiated power components by fitting VUV and XUX line intensities to the total radiated power /4/, has now been extended to the soft x-ray spectroscopic data. It relies on observing ions whose line radiation has been found empirically to represent the radiated power from the relevant impurity, and on analysing a large number of discharges to ensure consistency of the fitting coefficients. In the VUV and soft x-ray regions, the most suitable ionisation stages have been found to be H-like for Be, C, and O, Li-like for Cl, and Be-like for Cr, Fe and Ni.

During the first half of 1994 operations, the condition of the machine was monitored using regular reference discharges. Figure 3 shows the elemental radiated power components together with their sum and total radiated power for such a discharge. The plasma was formed on the outboard limiter, was then moved to an X-point magnetic configuration, followed by phases on the outboard and inboard limiters, thereby allowing the condition of each surface to be assessed /5/. The evolution of the main impurities during a series of reference discharges (fig.4) shows that the most significant change occurs to Cl. At the start of operations in 1994, Cl was a major radiator, but after about 1000 discharges it had declined to negligible levels, while briefly returning after each vessel opening. This is probably due to gettering by the metals, which have been shown to be anticorrelated with Cl /6/.

A useful guide to the general impurity radiation is to normalise the average Ohmic P_{rad} to the current I_p (table 1). The level of $<P_{rad}/I_p>$ for the first half of 1994 (0.23MW/MA) was very similar to that for equivalent discharges in 1989 (0.22MW/MA). As in the 1989 C-limiter/Be-evaporation phase, C is the major low-Z radiator, and Be is at very low levels except for a few shots following a Be evaporation. Ni, Fe and Cr are higher with the new configuration, mainly due to the larger area of exposed vacuum vessel, than in 1990/92, when the walls had a larger covering of carbon tiles. An all-shot survey of the P_{rad} components of Be, and O (fig.5) shows the Be trend after Be evaporations. There is a general downward trend in O, as well as short-lived decreases after each evaporation.

Table 1. Comparison of $<P_{rad}/I_p>$, first-wall material, and major radiating impurities, for recent years' operations.

Start of operations	$<P_{rad}/I_p>$ (MW/MA)	First-wall material	Main radiating impurities
1987	0.41	C, Ni antenna screens.	C, O, Ni.
1989	0.30	C.	C, Cl, Ni, O.
1989	0.22	C, Be evaporation.	C, Cl, Ni, Be.
1990	0.18	C/Be.	Be, C, Cl.
1991	0.20	C/Be.	Be, C, Cl, Ni.
1994	0.23	C, Be evaporation.	C, Cl, Ni, Fe, Cr.

The bulk-impurity line-intensities from Ohmic X-point plasmas are significantly lower than from limiter plasmas particularly for the light impurities, for a combination of possible reasons, including global density changes, T_e and n_e profile changes, and divertor screening. For example, the reduction during the X-point phase of the reference discharge (fig.3) is believed to be mainly due to the reduction in density caused by increased pumping by the carbon divertor target. Impurity time histories (fig.6) for a high performance H-mode discharge with 19MW of NBI show marked decreases in the CIV and OV signals during the transition to X-point. In this case the reduction may be mainly a profile effect, where the light ions move into regions of lower n_e. The decrease is less pronounced for the more central NiXXVI ion, whose intensity then rises during the ELM-free period, with sharper increases at the occurence of giant ELMs. Further analysis is required to isolate the above effects in this data.

Conclusion

The use of absolutely-calibrated soft x-ray spectra, combined with code modelling, has allowed a comparison between passive and CXRS measurements. The technique of deriving impurity radiated power components has been valuable for the analysis of long sequences of discharges. The total radiated power is similar to previous years, particularly when comparable first-wall materials were used. After a long series of discharges, while there are often exceptions, C is the major low-Z radiator, Be and O are low, Cl is negligible, while radiation from Ni, Fe and Cr is higher.

1. R Barnsley et al, Rev. Sci. Instrum. **57**(8) (1986) 2159.
2. R Barnsley et al, Rev. Sci. Instrum. **63**(10) (1992) 5023.
3. N J Peacock et al, Rev. Sci. Instrum. **66**(2) (1995) 1175.
4. K D Lawson et al, 17th EPS Amsterdam (1990).
5. G Saibene, A Rossi et al. J. Nucl. Mat. 220-222 (1995) 617-622.
6. K D Lawson, N J Peacock. AEA Culham Report. TAN-92-1-5, (1992).

HC was supported by IAEA fellowship (CPR/94004P) through AEA.

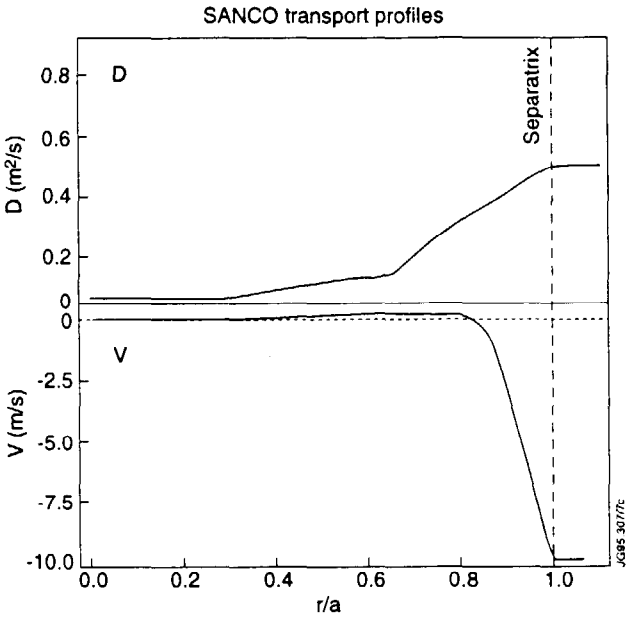

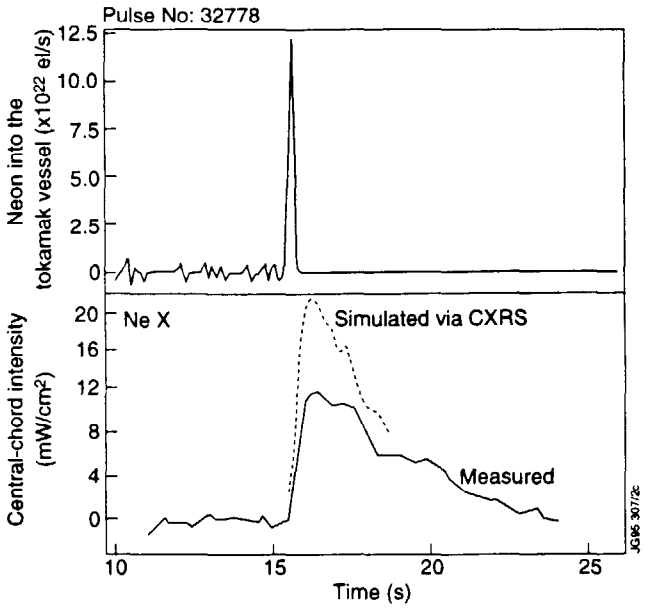

Figure 1. (left) Radial profiles of transport coefficients D and V, determined by modelling the CXRS Carbon and Neon profiles. **Figure 2.** (right) Simulated Ne X Lyβ derived from CXRS, compared with the independently calibrated soft x-ray spectroscopic measurement.

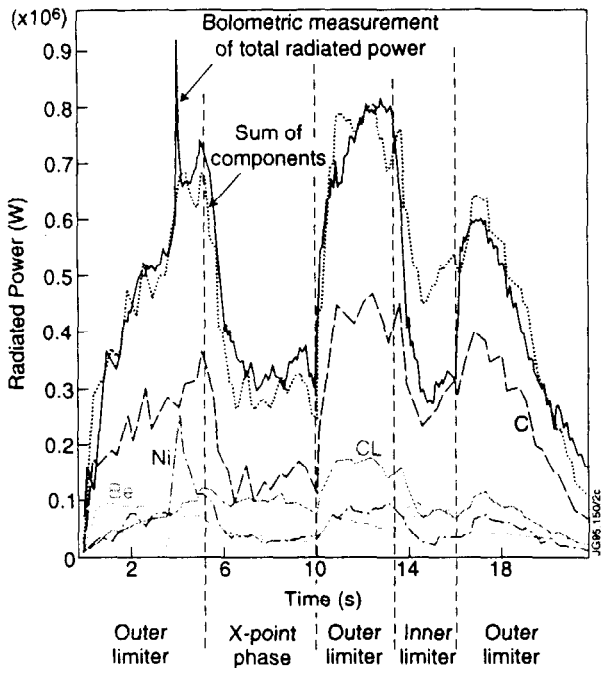

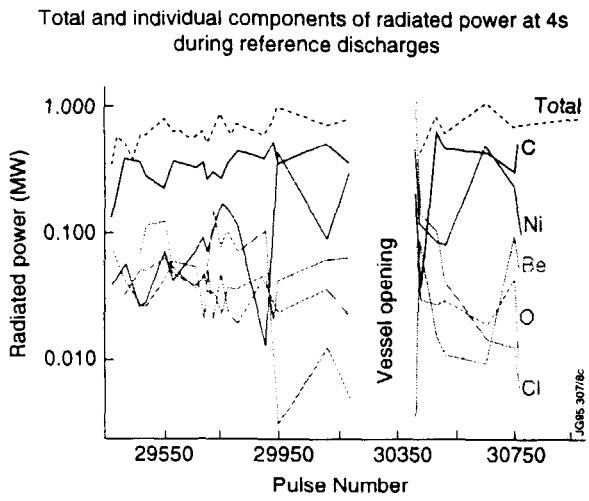

Figure 3. (left) A fit of the soft x-ray spectroscopic line intensities to the total radiated power, for a reference discharge. **Figure 4.** (right) Total radiated power and main impurity components, measured during the outer limiter phase of a series of reference discharges.

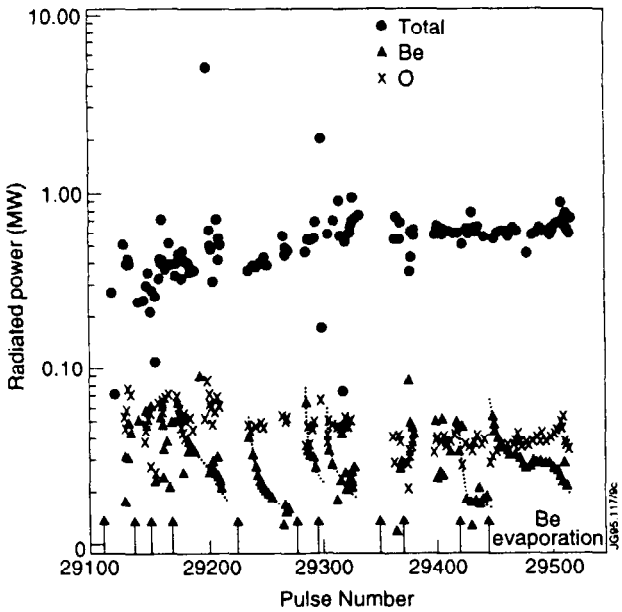

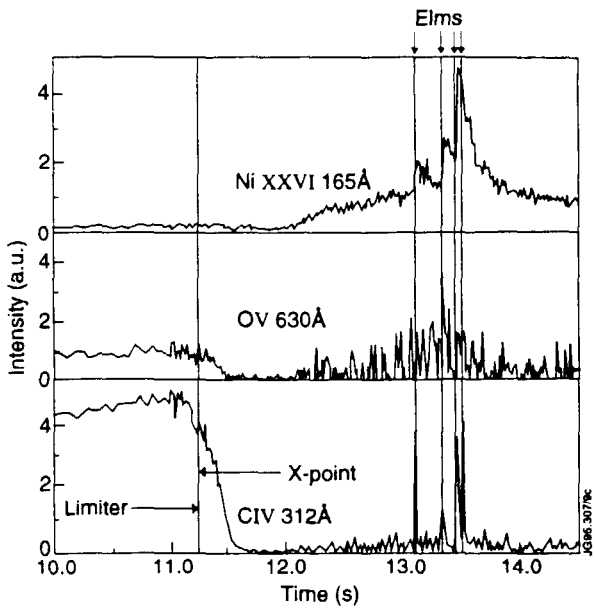

Figure 5. (left) Total, beryllium and oxygen radiated power at 4s for a series of discharges. Dotted lines indicate the trend after beryllium evaporations **Figure 6** (right) Time histories of three representative VUV lines for a high performance discharge.